Resource

Cell Reports

Large-Scale Arrayed Analysis of Protein Degradation Reveals Cellular Targets for HIV-1 Vpu

Graphical Abstract

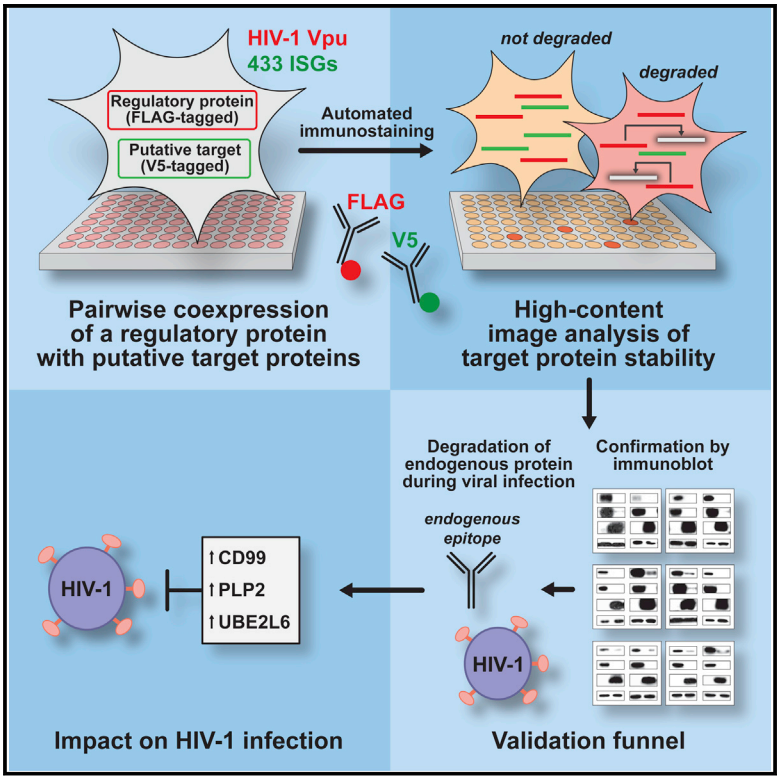

Highlights

- Developed proteomics platform to enable the arrayed analysis of protein stability
- Proof-of-concept application identified cellular targets of HIV-1 Vpu
- Vpu degrades cellular E2 ligase UBE2L6 to inhibit global conjugation of ISG15
- CD99 and PLP2 interfere with packaging of HIV-1 envelope and are targeted by Vpu

Authors

Prashant Jain, Guney Boso, Simon Langer, ..., Sunnie M. Yoh, Lars Pache, Sumit K. Chanda

Correspondence

lpache@sbpdiscovery.org (L.P.), schanda@sbpdiscovery.org (S.K.C.)

In Brief

Retroviruses use their accessory proteins to evade immune detection and enhance viral replication. Jain et al. developed a high-throughput–high-content imaging platform to study protein stability and degradation. This method was then applied to reveal cellular targets of the HIV-1 accessory factor Vpu.

Jain et al., 2018, Cell Reports 22, 2493–2503
February 27, 2018
https://doi.org/10.1016/j.celrep.2018.01.091

CellPress

Cell Reports
Resource

Large-Scale Arrayed Analysis of Protein Degradation Reveals Cellular Targets for HIV-1 Vpu

Prashant Jain,[1,2,4] Guney Boso,[1,2,5] Simon Langer,[1] Stephen Soonthornvacharin,[1,6] Paul D. De Jesus,[1] Quy Nguyen,[1,7] Kevin C. Olivieri,[1,8] Alex J. Portillo,[1] Sunnie M. Yoh,[1] Lars Pache,[1,3,*] and Sumit K. Chanda[1,3,9,*]
[1]Sanford Burnham Prebys Medical Discovery Institute, 10901 North Torrey Pines Road, La Jolla, CA 92037, USA
[2]These authors contributed equally
[3]Senior author
[4]Present address: University of California, San Diego, La Jolla, CA, USA
[5]Present address: National Institute of Allergy and Infectious Diseases, Bethesda, MD, USA
[6]Present address: Tocagen, Inc., San Diego, CA, USA
[7]Present address: Kyowa Kirin Pharmaceutical Research, Inc., La Jolla, CA, USA
[8]Present address: Homology Medicines, Inc., Bedford, MA, USA
[9]Lead Contact
*Correspondence: lpache@sbpdiscovery.org (L.P.), schanda@sbpdiscovery.org (S.K.C.)
https://doi.org/10.1016/j.celrep.2018.01.091

SUMMARY

Accessory proteins of lentiviruses, such as HIV-1, target cellular restriction factors to enhance viral replication. Systematic analyses of proteins that are targeted for degradation by HIV-1 accessory proteins may provide a better understanding of viral immune evasion strategies. Here, we describe a high-throughput platform developed to study cellular protein stability in a highly parallelized matrix format. We used this approach to identify cellular targets of the HIV-1 accessory protein Vpu through arrayed coexpression with 433 interferon-stimulated genes, followed by differential fluorescent labeling and automated image analysis. Among the previously unreported Vpu targets identified by this approach, we find that the E2 ligase mediating ISG15 conjugation, UBE2L6, and the transmembrane protein PLP2 are targeted by Vpu during HIV-1 infection to facilitate late-stage replication. This study provides a framework for the systematic and high-throughput evaluation of protein stability and establishes a more comprehensive portrait of cellular Vpu targets.

INTRODUCTION

A primary mechanism by which lentiviruses, including HIV-1, evade innate immune restriction is through ubiquitination of host restriction factors, which leads in many cases to proteasome-mediated degradation (Rustagi and Gale, 2014; Strebel, 2013). Accessory proteins uniquely expressed by complex retroviruses are the predominant mediators of this immune evasion strategy. For example, the Vif protein of HIV-1 recruits the Cul5-Elongin ubiquitin ligase complex to target the antiviral interferon stimulated gene (ISG) APOBEC3G for degradation (Kobayashi et al., 2005; Marin et al., 2003; Sheehy et al., 2002), whereas Vpu directs the degradation of CD4 and BST2/tetherin (Neil et al., 2008; Van Damme et al., 2008; Willey et al., 1992). The HIV-2 and simian immunodeficiency virus (SIV)-encoded Vpx protein causes degradation of SAMHD1 to facilitate reverse transcription in myeloid and resting T cells (Hrecka et al., 2011; Laguette et al., 2011). A number of these lentiviral accessory protein targets were discovered in the context of specific cellular backgrounds that were found to be restrictive for accessory factor mutant viruses. However, numerous functional and protein-interaction studies have provided evidence that HIV-1 accessory proteins may target a broader set of cellular factors than is currently appreciated (Haller et al., 2014; Jäger et al., 2011; Matheson et al., 2015). Therefore, a systematic analysis of HIV-1 accessory protein-mediated degradation events may provide important new insights into additional viral evasion mechanisms.

Vpu has been well documented to promote viral replication and pathogenesis through antagonism of innate immune mechanisms (Roy et al., 2014). Most notably, Vpu has been reported to counteract BST2/tetherin (Neil et al., 2008; Roy et al., 2014; Van Damme et al., 2008) to facilitate efficient virion release, and CD4 (Willey et al., 1992) to prevent superinfection (Wildum et al., 2006) and boost the production of cell-free infectious virions (Lama et al., 1999). Additional documented Vpu targets that function in immune regulation include CD1d (Moll et al., 2010), natural killer, T, and B cell antigen (NTB-A) (Shah et al., 2010), CD155 (Matusali et al., 2012), CCR7 (Ramirez et al., 2014), and SNAT1 (Matheson et al., 2015). These data suggest that Vpu targets modulators of cell non-autonomous immune functions, in addition to direct regulators of viral replication. Given the diversity of the described Vpu targets, and complex mechanisms by which these proteins are inactivated (Dubé et al., 2011; Goffinet et al., 2009; Kueck and Neil, 2012; Lewinski et al., 2015), the complete scope of host proteins targeted by Vpu likely is not yet fully appreciated. Therefore, a comprehensive and unbiased analysis of host proteins modulated by Vpu would not only enhance our understanding of the critical cellular processes that facilitate viral replication but also shed light

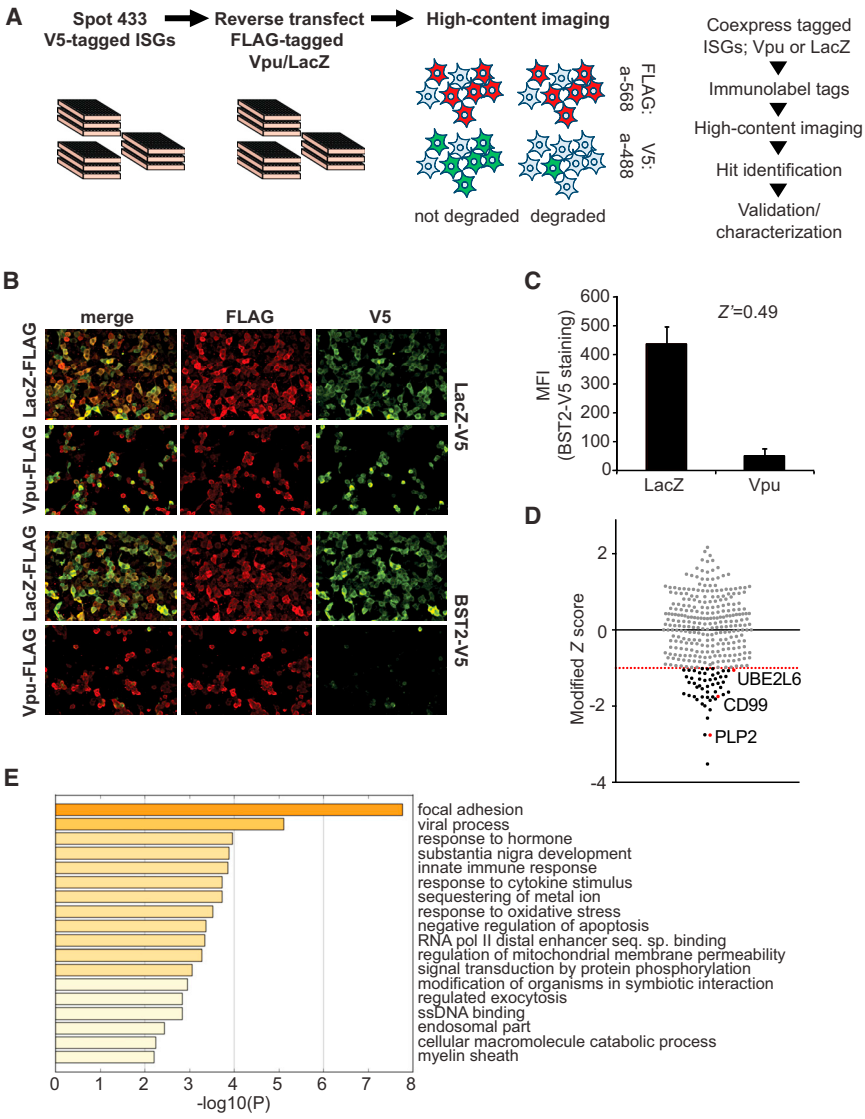

Figure 1. Global Arrayed Protein Stability Analysis

(A) Schematic representation of the Global Arrayed Protein Stability Analysis (GAPSA) platform.

(B) Representative images of fluorescently immunolabeled HEK293T cells coexpressing LacZ-FLAG or Vpu-FLAG (Alexa Fluor 568) with either BST2-V5 or LacZ-V5 (Alexa Fluor 488).

(C) Z' calculation for the loss of cellular BST2/tetherin levels following coexpression with Vpu-FLAG versus LacZ-FLAG. Data is shown as mean ± SD.

(D) Modified Z score indicating degradation of ISGs following Vpu expression relative to LacZ expression for all genes expressed in the screen that met the quality control criteria. Hits are highlighted in black and genes selected for functional characterization are shaded red. See Table S1 for screen data.

(E) Metascape-based Gene Ontology (GO) analysis of primary screen hits.

MFI, mean fluorescence intensity; ssDNA, single-stranded DNA.

on general strategies used by HIV-1 to facilitate immune evasion on a global scale.

In this study, we report the development of a high-content imaging platform, the Global Arrayed Protein Stability Analysis (GAPSA), which enables a highly parallelized analysis of protein stability at the level of the proteome. We assessed the performance of this platform by identifying cellular targets of Vpu using a cDNA matrix comprising 433 individual ISGs. Several previously unreported Vpu host targets were identified using this approach. Validation studies confirmed Vpu-dependent modulation of 26 host proteins by ectopic expression and immunoblot analysis. We further verified the Vpu-dependent downregulation of a subset of these factors in the context of viral infection, and functionally validated the antiviral activities of CD99, PLP2, and UBE2L6. Taken together, these data underscore the utility of the GAPSA platform to identify cellular factors that are targeted for degradation by specific proteins or cellular stimuli, and further establish a more extensive set of host factors that are modulated by Vpu.

RESULTS

High-Content Imaging-Based Screen for Vpu Targets

We developed GAPSA, a high-content imaging-based approach, to better understand the range of proteins that may be targeted for degradation by specific factors or extracellular stimuli. This platform enables the large-scale evaluation of changes in target protein levels following coexpression with a regulatory factor, or the addition of stimuli, in an arrayed format. Specifically, this methodology relies on high-throughput visualization of protein abundance following coexpression and differential fluorescent labeling. We assessed the efficacy of this approach towards identifying protein destabilization events directed by Vpu. Cells coexpressing V5-tagged BST2/tetherin and either Vpu-FLAG or a LacZ-FLAG control were immunostained in a 384-well format with anti-V5 and anti-FLAG antibodies, and secondary antibodies labeled with Alexa Fluor 488 and Alexa Fluor 568 fluorescent dyes, respectively. BST2/tetherin served as a positive control, and the analysis was conducted in duplicate. To ensure consistent immunostaining of expressed V5 and FLAG epitopes in all wells and between plates, an automated protocol was developed to wash, fix, permeabilize, and immunolabel each sample (Figure 1A; Supplemental Experimental Procedures). Cells coexpressing BST2/tetherin and LacZ showed a robust staining intensity, whereas a significant loss of BST2/tetherin staining intensity was observed in cells expressing Vpu-FLAG (Figures 1B and 1C). We determined a Z' score of 0.49 for the assay, indicating a suitable window for this automated screening approach (Figure 1C).

In this study, we used the GAPSA platform to identify cellular targets of the HIV-1 accessory protein Vpu by coexpressing 433 V5-tagged putative ISGs, selected based on previous publications (Barr et al., 2008; Der et al., 1998; Goujon et al., 2013; Kane et al., 2016; Rusinova et al., 2013; Waddell et al., 2010) and availability within the human ORFeome V8.1 library (Yang et al., 2011). Baseline expression levels were established by assessing the protein abundance of each ISG after cotransfection with a LacZ control. Following automated analysis of the image output, Vpu-dependent changes of ISG protein levels were determined as the ratio between mean fluorescence intensity (MFI) of V5 (ISG) staining in cells coexpressing Vpu and those coexpressing LacZ. Of the initial set of 433 genes, 321 ISGs showed robust expression, defined as 3 times above background staining intensity, in each of the replicate samples and were further considered for downstream analysis. Fold changes in V5 staining intensities of Vpu-expressing cells were calculated relative to LacZ-expressing control cells, and median fold changes were determined for data collected from each plate within the screen. Modified *Z* scores were calculated using the plate median and the median absolute deviation (MAD) for each gene (Salgado et al., 2016). Primary hits were identified as genes that showed a modified *Z* score below −1.0. Based on these criteria, we identified 52 proteins as putative Vpu targets (Figures 1D and S1; Table S1).

To understand the enrichment of biological and cellular processes among these hits, we applied a Gene Ontology (GO) analysis using the Web-based tool Metascape (www.metascape.org) (Tripathi et al., 2015) (Figure 1E). This analysis revealed significant enrichment of, among others, genes involved in focal adhesion (Figure 1E). Among these were CFL1, a protein that depolymerizes F-actin and that, upon knockdown, was shown to enhance transinfection of HIV-1 between dendritic cells (DCs) and T lymphocytes (Ménager and Littman, 2016); CD99, which is involved in T cell adhesion and leukocyte migration (Bernard et al., 2000; Hahn et al., 1997; Sohn et al., 2001); and ATP1B1, which is a subunit of the Na^+/K^+ transporter. These results suggest that Vpu-mediated immune evasion strategies may affect a broader range of host cell functions than previously appreciated, including host metabolic processes and plasma membrane activities.

Validation of Vpu-Dependent Downregulation of ISGs

Vpu-dependent downregulation of screen hits was validated by immunoblot analysis of ISG protein levels following coexpression with FLAG-tagged Vpu or LacZ in HEK293T cells. To avoid plate bias in selecting factors, we chose 38 proteins, which included up to 10 hits per plate, prioritized by modified *Z* score values. Of the 38 selected ISG hits, 33 showed detectable protein levels in the immunoblot-based validation assay and these were evaluated for protein degradation upon Vpu coexpression. We confirmed a Vpu-dependent reduction of protein levels for 26 of the 33 ISGs (Figures 2A and S2A), representing a confirmation rate of 79%. Of the 26 validated genes, 13 were strongly downregulated (>75% reduction), 6 were moderately downregulated (between 75% and 50% reduction), and 7 were weakly downregulated (between 50% and 25% reduction). Among the validated factors, only 3 genes showed a >25% reduction in mRNA transcript levels, indicating that the differences in protein levels following Vpu coexpression were not predominantly the result of transcriptional regulation (Figure S2B).

Functional Characterization of Identified Vpu Targets

Next, we evaluated the effect of ISG overexpression on HIV-1 infectivity. Toward this end, we transfected HEK293T cells with wild-type (WT) (HIV-1-Luc) and Vpu-deficient (HIV-1-ΔVpu-Luc) proviral DNA and cotransfected 17 of the 26 validated hits (see Supplemental Experimental Procedures for selection criteria). Supernatants were harvested 72 hr post-transfection and used to infect HEK293T.CD4.CCR5 cells. Overexpression of 15 of the 17 hits led to a reduction in viral infection compared to the LacZ control (Figure 2B). Moreover, overexpression of 11 of the 15 ISGs affected the infection of Vpu-deficient virus to a significantly greater extent than WT virus. We hypothesize that the proteins that are targeted for degradation by Vpu, but do not affect replication, may affect non-cell autonomous processes such as immune effector functions, or they may be "bystander" targets of Vpu, and their removal may not provide an advantage for viral replication.

Evaluation of Proteasome and HIV Accessory Protein Dependence of ISG Degradation

It has been observed that Vpu-dependent degradation of host factors involves, at least in some cases, proteasome-mediated degradation in an Skp, Cullin, F-box β-transducin repeat-containing protein ($SCF^{\beta\text{-}TrCP}$)-dependent manner (Magadán et al., 2010; Mitchell et al., 2009; Willey et al., 1992). To determine whether proteasomal activity is required for the Vpu-dependent degradation of the identified factors, cellular expression levels of 10 Vpu targets (Figure 2A), whose expression also resulted in a significant reduction of reporter virus infection (Figure 2B), were evaluated in the presence or absence of the proteasome inhibitor MG132 (Figures 2C and S3A). Treatment with MG132 rescued the Vpu-dependent reduction of CD99, LIPG, and UBE2L6 >2-fold (strong rescue), and of IL1RN and CFL1 between 1.2- and 1.4-fold (moderate rescue). The protein levels of the remaining targets were not rescued upon MG132 treatment, suggesting that Vpu is mediating their degradation in a proteasome-independent manner.

Next, we investigated the ability of additional HIV-1 and -2 accessory proteins to regulate the protein levels of the 10 ISGs described above. We found that the protein degradation of most factors was mediated primarily by Vpu (Figures 2D and S3B). However, LIPG protein levels also were reduced upon coexpression with the HIV-1 accessory protein Vif, and ARID3B was downregulated by the HIV-2 accessory protein Vpx. These data suggest a certain level of redundancy in specificity for some host cell targets between multiple HIV-1 accessory proteins, which is consistent with previous studies (Haller et al., 2014; Matheson et al., 2015).

To determine the level of false-positive hit identification resulting from ectopic protein expression in the GAPSA system, we further assessed changes in the endogenous levels of 7 proteins that include factors that showed substantial downregulation by Vpu, significantly decreased viral infection upon overexpression (Figure 2B), or both. Vpu expression clearly reduced

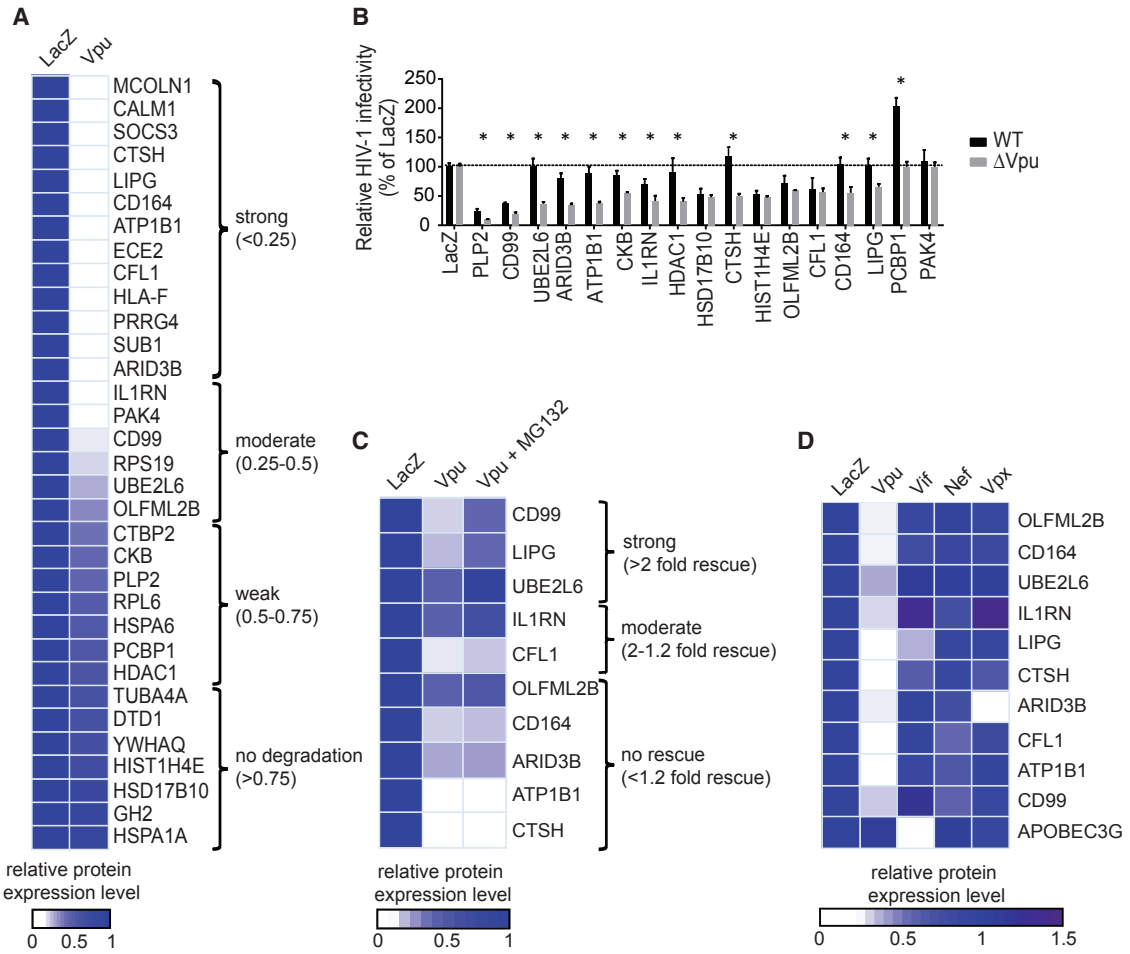

Figure 2. Hit Validation and Functional Evaluation of Putative Vpu Targets

(A) Heatmap representing relative fold change of putative target protein levels following Vpu expression. Data are derived from densitometric analysis of immunoblots of whole-cell lysates of HEK293T cells coexpressing Vpu-FLAG or LacZ-FLAG with the indicated V5-tagged ISGs. Data represent average fold change from 2 independent experiments. See Figure S2A and Table S1 for detailed immunoblot results.

(B) HIV-1-Luc or HIV-1-ΔVpu-Luc produced in HEK293T cells ectopically expressing a subset of selected hits, or LacZ as control, was used to infect HEK293T.CD4.CCR5 cells. Normalized Renilla luciferase reporter values are shown relative to LacZ control (100%). (*) Factors that inhibited infectivity of HIV-1-ΔVpu-Luc significantly greater than WT ($p \leq 0.05$). Data are represented as mean ± SEM.

(C) Heatmap representing fold change of Vpu target protein levels in western blots following Vpu expression, relative to LacZ expression, in whole-cell lysates of HEK293T cells in the presence or absence of MG132. The proteasome dependence of the ISG degradation was designated as "strong" (>2-fold rescue) or "moderate" (2- to 1.2-fold rescue). Data represent average fold change from 2 independent experiments. See Figure S3A for representative immunoblots.

(D) Heatmap representing fold change in protein expression levels determined by western blot following expression of Vpu, Vif, Nef, and Vpx, relative to LacZ expression in whole-cell lysates of HEK293T cells. Data represent average fold change from 2 independent experiments. See Figure S3B for representative immunoblots.

endogenous protein levels of 6 of the 7 proteins (Figure 3A). Next, we determined whether the factors were targeted for Vpu-dependent degradation in the context of viral infection. We assessed the degradation of CD99, ARID3B, and PLP2 upon infection of either WT or Vpu-deficient HIV-1 with comparable titers. These data showed considerable decreases in endogenous levels of CD99, ARID3B, and PLP2 following infection with WT HIV-1, in contrast to minor changes with a Vpu-deficient strain (Figure 3B). Although additional studies are necessary to comprehensively evaluate the degradation and functional effects of the factors identified by our screen, these data demonstrate that the GAPSA system is able to successfully identify endogenous host cell factors that are degraded by an HIV-1 accessory protein upon viral infection.

Vpu Inhibits the Conjugation of ISG15 to Cellular Proteins through Targeting of UBE2L6

In addition to the factors described above, we found that UBE2L6, an E2 ligase essential for the conjugation of ISG15 to host proteins (ISGylation) that mediates broad post-translational modifications of several host and microbial proteins (Zhang and Zhang, 2011), is degraded specifically by Vpu. Notably,

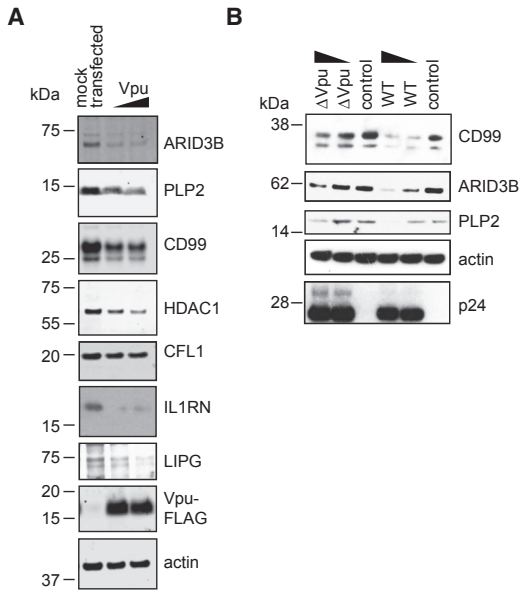

Figure 3. Vpu-Dependent Degradation of Endogenous ISGs

(A) Whole-cell lysates of HeLa cells transiently overexpressing Vpu were probed with the indicated antibodies.

(B) Immunoblots of THP-1 cells infected with WT or Vpu-deficient strains of HIV-1 were probed with the indicated antibodies. Actin levels were used as loading control, and Gag-p24 levels indicate viral infection levels.

All data are representative of 2 independent experiments.

ISGylation has been directly implicated in impeding HIV-1 budding and egress (Pincetic et al., 2010). We therefore investigated whether Vpu-dependent degradation of UBE2L6 affects the global ISGylation levels of proteins in infected THP-1 cells (Figure 4A), primary monocyte-derived macrophages (MDMs) (Figure 4B), and HeLa cells (Figure S4A). Cells were infected with either WT or Vpu-deficient HIV-1 at comparable titers. Interferon β (IFNβ) was added to cells 24 hr before harvesting to upregulate expression of the ISGylation machinery. Immunoblotting analysis showed a considerable decrease in ISG15 conjugates and endogenous UBE2L6 levels following WT HIV-1 infection as compared to the uninfected control. Notably, infection with Vpu-deficient HIV-1 resulted in endogenous UBE2L6 and ISG15 conjugation levels comparable to, or higher than, uninfected cells. These findings suggest that HIV-1 reduces global ISGylation levels in a Vpu-dependent manner. We further evaluated whether expression of Vpu alone was sufficient to downregulate ISGylation independently of viral infection. We observed a marked decrease in ISG15 conjugates in cells overexpressing Vpu compared to non-transfected or Nef-overexpressing cells (Figure 4C). These data demonstrate that expression of Vpu is sufficient to downregulate global ISGylation mechanisms in cells.

Because ISGylation has been reported to inhibit HIV-1 budding and release (Okumura et al., 2006; Pincetic et al., 2010; Woods et al., 2011), we evaluated the role of UBE2L6 in HIV-1 late-stage replication. We observed >65% inhibition of virion release 72 hr post-infection in UBE2L6-expressing cells as compared to cells expressing the vector control. UBE2L6-mediated inhibition of virion release was more pronounced in cells infected with Vpu-deficient virus as compared to cells infected with the WT virus, indicating that Vpu counteracts the antiviral effects mediated by UBE2L6 (Figure 4D). Because we did not observe a difference in viral luciferase reporter activity between UBE2L6-expressing cells and control cells, we concluded that the impact of UBE2L6 on virion release was not caused by differences in viral input or gene expression (Figure S4B). We also observed that small interfering RNA (siRNA)-mediated knockdown of UBE2L6 in THP-1 cells resulted in enhanced HIV-1 production (Figures 4E and S4C), further supporting a negative regulatory effect of this factor on viral replication.

Evaluation of Antiviral Functions of CD99 and PLP2

Our experiments showed that overexpression of CD99 and PLP2 in producer cells resulted in an up to 10-fold reduction in the infectivity of reporter virus in a Vpu- and dose-dependent manner (Figures 2B and 5A). Importantly, p24 levels in the supernatant of producer cells were not affected by the overexpression of these genes (Figure S5), indicating that the impact of these proteins on viral replication occurs after viral egress. Infectivity of virions produced in the presence of CD99 and PLP2 was similarly tested in primary $CD4^+$ T cells, in which we also observed a drastic decrease in virion infectivity upon overexpression of CD99 and PLP2 (Figure 5B).

To investigate the potential effects of CD99 and PLP2 on the viral life cycle steps that occur after the first round of infection, we infected HEK293T cells that express the HIV-1 receptor and co-receptor (HEK293T.CD4.CCR5) with viruses that were produced in the presence of CD99, PLP2, or LacZ. Bound and unbound virions that failed to enter the cells were removed by trypsin treatment 3 hr post-infection, followed by extensive washes. Immunoblotting analysis showed that cells infected with virus produced in the presence of ectopically expressed CD99 or PLP2 contained reduced amounts of the viral capsid protein p24 (Figure 5C). It is interesting that these virions contained an excess amount of unprocessed gp160 (Figure 5D), whereas the HEK293T cells used to produce these viral particles did not show increased gp160 levels, indicating that excess gp160 packaging into virions is not the result of a defect in viral envelope processing in the cells (Figure 5E). These results indicate that expression of both CD99 and PLP2 leads to production of HIV-1 particles that are defective in viral entry/binding, and suggest that Vpu targets these proteins to promote viral replication.

DISCUSSION

Subversion of antiviral mechanisms by HIV-1 critically depends on the ability of HIV-1 accessory proteins to degrade specific host targets in the cell. Importantly, several of the confirmed Vpu targets identified in this study are associated with known antiviral activities, as described below. Ontology analysis of our screening data found an enrichment of genes that are involved in processes such as focal adhesion (GO: 0005925), viral processes (GO: 0016032), innate immune responses (GO: 0045087), and the response to cytokine stimuli (GO: 0071345)

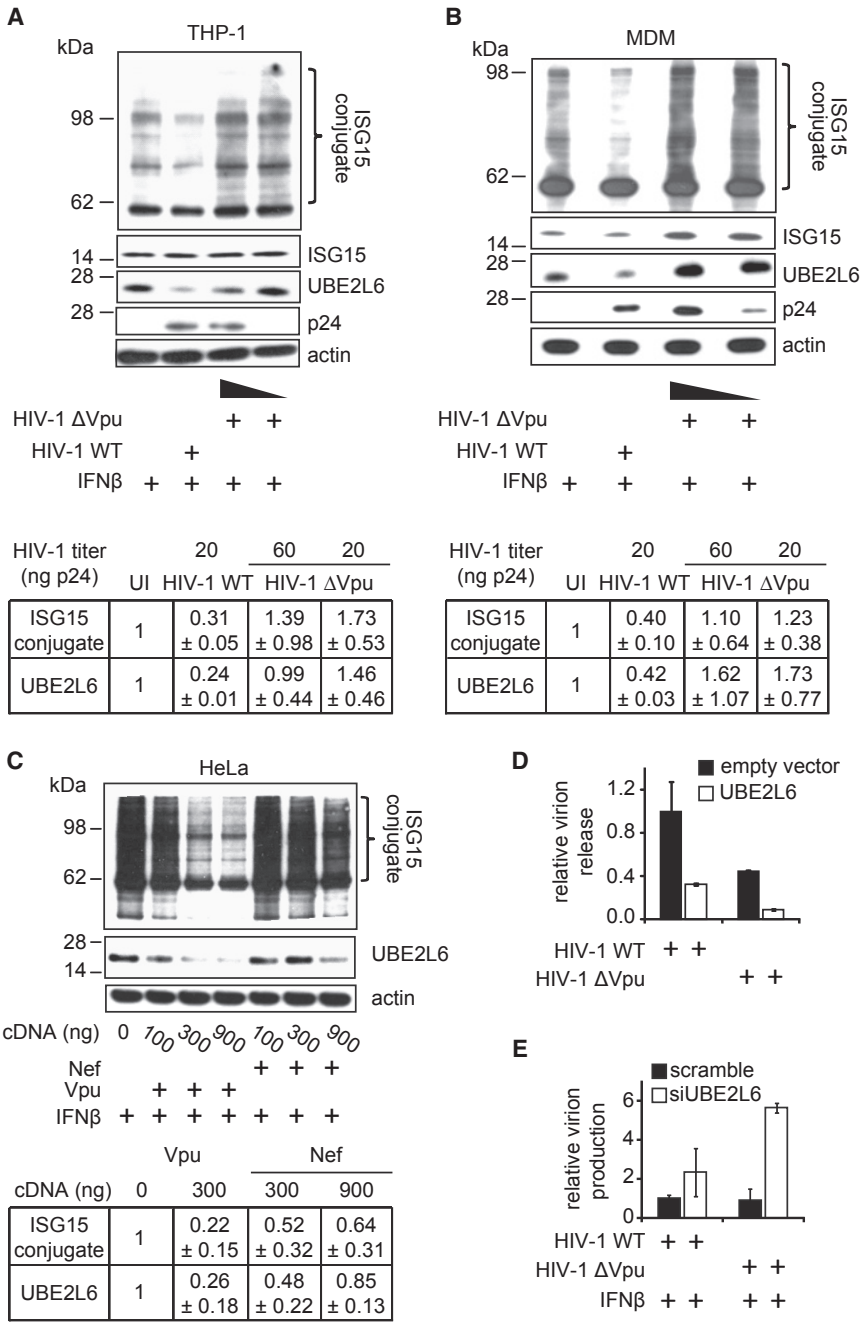

HIV-1 titer (ng p24)	UI	20 HIV-1 WT	60 HIV-1 ΔVpu	20 HIV-1 ΔVpu
ISG15 conjugate	1	0.31 ± 0.05	1.39 ± 0.98	1.73 ± 0.53
UBE2L6	1	0.24 ± 0.01	0.99 ± 0.44	1.46 ± 0.46

HIV-1 titer (ng p24)	UI	20 HIV-1 WT	60 HIV-1 ΔVpu	20 HIV-1 ΔVpu
ISG15 conjugate	1	0.40 ± 0.10	1.10 ± 0.64	1.23 ± 0.38
UBE2L6	1	0.42 ± 0.03	1.62 ± 1.07	1.73 ± 0.77

		Vpu	Nef	
cDNA (ng)	0	300	300	900
ISG15 conjugate	1	0.22 ± 0.15	0.52 ± 0.32	0.64 ± 0.31
UBE2L6	1	0.26 ± 0.18	0.48 ± 0.22	0.85 ± 0.13

Figure 4. Evaluation of HIV-1 Infection-Dependent Modulation of Cellular ISGylation Mechanism and Functional Validation of UBE2L6

(A and B) Immunoblotting analysis of THP-1 cells (A) and monocyte derived macrophages (MDMs) (B) infected with WT (HIV-1-VSV-G) or Vpu-deficient (HIV-1-ΔVpu-VSV-G) virus. IFNβ was added 2 days after infection. See Figure S4A for Vpu-dependent downregulation of ISGylation in HeLa cells.

(C) Immunoblotting analysis of HeLa cells transfected with the indicated concentrations of either FLAG-tagged Vpu or Nef for 2 days. IFNβ was added 1 day post-transfection. Corresponding pixel intensities of ISG15 and UBE2L6 bands, averaged from 2 independent experiments, are shown below the blots, ± SD.

(D) Relative Gag p24 levels in culture supernatant from THP-1 cells stably expressing UBE2L6 or a vector control that were infected with WT or Vpu-deficient HIV-1. Error bars indicate SD. See also Figure S4B.

(E) Relative changes in virus replication, as determined by luciferase gene expression, in THP-1 cells following siRNA knockdown of UBE2L6 versus scrambled siRNA control. See also Figure S4C. Error bars indicate SD.

All data are representative of 2 independent experiments. siUBE2L6, small interfering RNA targeting UBE2L6.

Vpu-mediated degradation of ATP1B1 may enhance HIV-1 release through the regulation of plasma membrane depolarization. In addition, CD164 (endolyn) overexpression reduced the infection of a Vpu-deficient virus by 45% (Figure 2B) and was shown to restrict HIV-1 virion production in HEK293T cells upon overexpression (McLaren et al., 2015). Furthermore, both HIV-1 Nef and Vpu were found to downregulate the cell surface expression of CD164 in transfected immortalized T cells (Haller et al., 2014). Several genes involved in the regulation of focal adhesions and cell-cell junctions, including CFL1 and CD99, also were identified in our study. These results are consistent with the ability of Vpu to affect (Figure 1E). Several factors within these categories, when overexpressed during the production of a Vpu-deficient virus, were able to restrict viral infection (Figure 2B). Among these factors is ATP1B1, a protein vital for ATPase function and ion exchange across membranes within cells. Notably, several proteins involved in the ATP synthase complex were found to bind Vpu in a global HIV-1-host interaction study (Jäger et al., 2011). Moreover, depolarization of the resting cell membrane potential has been proposed to enhance a Vpu-dependent release of HIV-1 from cells (Hsu et al., 2010), suggesting that cellular actin dynamics and intercellular barrier integrity. Specifically, disruption of cell-cell junctions following HIV-1 infection has been reported (Nazli et al., 2010) and has been proposed to facilitate the paracellular spread of HIV-1 (Sufiawati and Tugizov, 2014). It is interesting that CD99 also was shown recently to be downregulated following Vpu expression by a stable isotope labeling with amino acids in cell culture (SILAC)-based mass spectrometry dataset (Sugden et al., 2017).

Vpu-dependent degradation of certain host factors has been shown to occur in an $SCF^{\beta\text{-}TrCP}$-dependent manner (e.g., CD4,

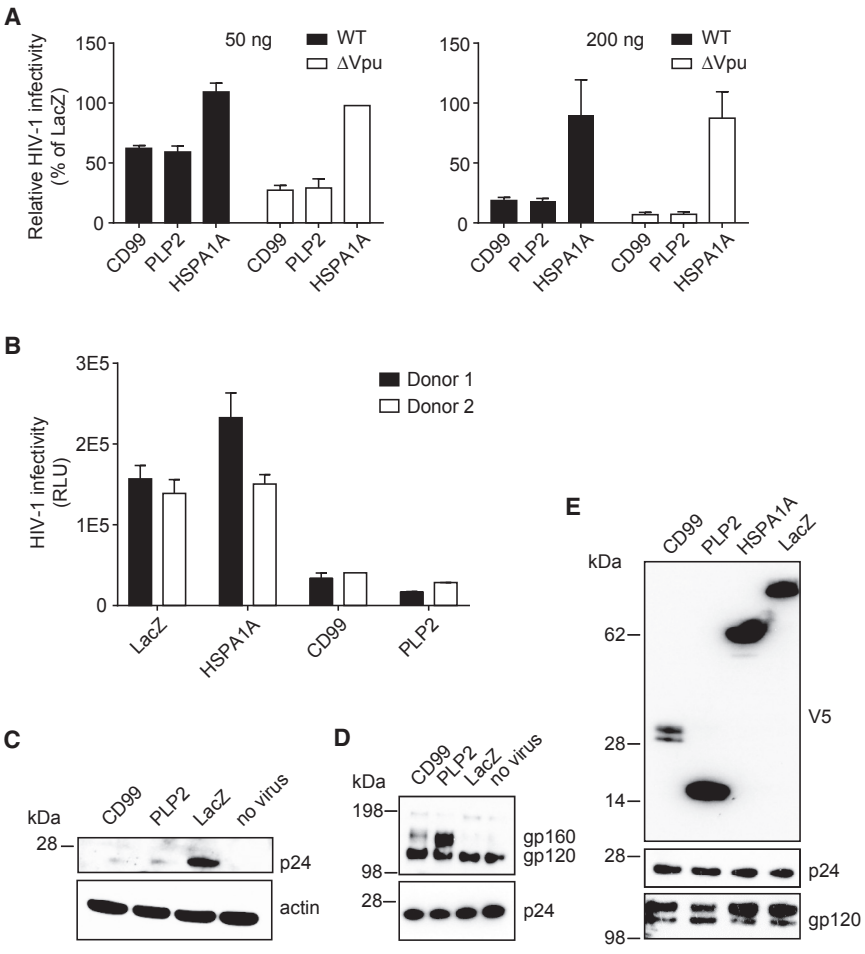

Figure 5. Ectopic Expression of CD99 and PLP2 Causes Production of Viral Particles Defective in Entry/Binding

(A) HIV-1-Luc or HIV-1-ΔVpu-Luc produced in HEK293T cells following transfection with 50 or 200 ng cDNA expressing LacZ, HSPA1A, CD99 or PLP2 was used to infect HEK293T.CD4.CCR5 cells. Normalized Renilla luciferase reporter values are shown relative to LacZ control (100%). See also Figure S5.

(B) $CD4^+$ T cells from 2 donors were infected with 15 pg p24 equivalent HIV-1-Luc produced in the presence of 200 ng of the indicated cDNAs. Renilla luciferase levels are shown. Error bars indicate SEM.

(C) HIV-1, produced in the presence of ectopically expressed LacZ, HSPA1A, CD99, or PLP2, was used to infect HEK293T.CD4.CCR5. Infected cells were lysed and analyzed by immunoblot 3 hr post-infection.

(D) Immunoblot analysis of viral lysates of HIV-1-Luc produced in the presence of the indicated genes that were ectopically expressed in HEK293T cells.

(E) Immunoblot analysis of whole-cell lysates derived from HEK293T cells cotransfected with HIV-1-Luc and cDNAs encoding the indicated genes.

All data are representative of 2 independent experiments. RLU, relative luminescence unit.

SNAT1). We find it interesting that approximately half of the Vpu targets queried were found to be degraded in a proteasome-dependent manner (Figures 2C and S3A). In addition to proteasome-dependent mechanisms, Vpu has been described to downregulate expression levels of cellular targets by proteasome-independent mechanisms, such as endolysosomal degradation (e.g., BST2) (Blanchet et al., 2012; Matheson et al., 2015), and Cullin RING ligase (CRL)-dependent mechanisms (Ramirez et al., 2015). Vpu also has been shown to modulate the anterograde trafficking that results in retention in the *trans*-Golgi network (TGN) (e.g., NTB-A, CCR7) (Bolduan et al., 2014; Ramirez et al., 2014; Shah et al., 2010), or to suppress membrane recycling pathways through the retention of cargo in early endosomes (e.g., CD1d) (Moll et al., 2010). Further investigations into the Vpu-dependent downregulation of ISGs identified in the present study will aid significantly in the understanding of proteasome-independent mechanisms used by Vpu to facilitate the evasion of cellular immune responses.

Our study identified 15 Vpu targets, which upon overexpression significantly reduced the infectivity of Vpu-deficient virus (Figure 2B). Of these identified genes, CD99 and PLP2 overexpression resulted in an up to 10-fold reduction in the infectivity of released HIV-1 particles in a Vpu-dependent manner. It is interesting that enhanced incorporation of unprocessed gp160 was observed in HIV-1 particles produced in cells overexpressing CD99 or PLP2 (Figure 5D). Incorporation of mature envelope (Env) in nascent virions involves the directed trafficking of Env molecules via the secretory pathway from the TGN to distinct Gag assembly sites in the plasma membrane (Muranyi et al., 2013). It has been suggested that the level of Env protein on the surface of budding virions may be maintained at a lower density to prevent the exposure of Env to immune surveillance mechanisms (Groppelli et al., 2014). Only a small percentage of gp160 is normally processed, whereas the rest is trafficked to lysosomes for degradation (Willey et al., 1988). The enhanced incorporation of unprocessed Env in progeny virions, which was observed in our study, likely is the result of deregulated Env trafficking, because we did not observe substantial differences in Env expression or processing in producer cells (Figure 5E). Both CD99 and PLP2 have been shown to regulate trafficking from the TGN to the cell surface (Sohn et al., 2001; Timms et al., 2013); therefore, it is conceivable that these proteins also potentiate the trafficking of Env, including unprocessed gp160, toward virion assembly sites in the plasma membrane. The mode of action proposed here is distinct from the mechanism of other host factors, such as IFITM2 and IFITM3, that have been shown to interact directly with Env in the producer cells and prevent Env processing (Yu et al., 2015). Additional studies on the impact of endogenous CD99 and PLP2 expression on virus replication will provide further insight into the role

of these proteins in Env trafficking and assembly of viral particles.

Our study found a role for Vpu in the inhibition of the cellular ISGylation machinery. We identified UBE2L6, the primary E2 ligase for ISGylation, as a target of Vpu-mediated degradation. Consistent with a direct targeting of UBE2L6, we did not observe any decrease in ISG15 monomers upon HIV-1 infection, suggesting that the ISG15 conjugation machinery is affected specifically by Vpu (Figures 4A and 4B). Host protein ISGylation has been implicated in cellular activities that restrict HIV-1 infection. Specifically, studies have demonstrated that HERC5, the E3 ligase component of the ISGylation machinery, reduces HIV-1 virion production through the aggregation of Gag at viral assembly sites in the membrane, which is distinct from the mechanism involving free ISG15 that results in Gag aggregation in both membrane and cytosolic regions of the cell (Woods et al., 2011). Additional mechanisms such as the inhibition of Gag and Tsg101 interaction by ISG15 (Okumura et al., 2006) have been implicated in regulating late-stage HIV-1 replication. Thus, Vpu-mediated modulation of the cellular ISGylation apparatus is likely to affect multiple cellular mechanisms directed against HIV-1.

The GAPSA platform was developed as a high-content imaging-based arrayed analysis of cellular protein stability, and we have applied it toward the identification of host proteins whose cellular levels are reduced through concomitant expression of Vpu. Our results provide a deeper insight into host cell strategies that have evolved to restrict pathogen replication, and corresponding viral evasion strategies that enable transmission, systemic infection, and pathogenesis. This screening platform combines the robustness and sensitivity of immunostaining ectopically expressed factors in an arrayed format with the scalability of high-throughput automation and algorithm-based image analysis, and hence represents a powerful platform for the systematic analysis of protein levels on a global scale. The current configuration of the GAPSA platform can be used to identify targets of other microbial regulatory proteins, including additional lentiviral accessory factors, or assess the impact of extracellular ligands or stimuli on protein degradation. We anticipate a number of additional applications of this approach, including the identification of E3 ligases of specific protein substrates using an arrayed ubiquitin ligase library, the assessment of subcellular localization dynamics, or the binary interrogation of protein interaction/proximity using fluorescence resonance energy transfer (FRET)- or absolute protein expression (APEX)-based approaches (Lee et al., 2016; Matthews et al., 2012).

Alternative approaches for evaluating protein stability and global protein levels include quantitative proteomic approaches based on mass spectrometry (Chan et al., 2007; Matheson et al., 2015). Although such approaches can provide significant insight into the regulation of specific proteins under various experimental conditions, the extent of the proteome covered by mass spectrometry-based methods is inherently biased against less abundant proteins, or restricted by cell type-specific expression patterns for each protein (Chandramouli and Qian, 2009; Keshishian et al., 2007; Liebler and Zimmerman, 2013; Shi et al., 2012a, 2012b). In contrast, the GAPSA platform does not rely on relative levels of protein abundance or expression in specific cell types because the regulation of protein degradation is tested in a binary manner using an ectopic expression format. Thus, GAPSA enables a more sensitive approach to assess the impact of a regulatory protein or extracellular stimulus on the degradation of an arrayed set of putative targets. In addition to providing more sensitive detection of degradation events, GAPSA can be reconfigured to also identify the regulators that govern these degradation processes (e.g. E3 ligases). Of note, artifacts of protein overexpression or noise in the immunofluorescent detection system can lead to the identification of false-positive activities, a potential trade-off for the platform's enhanced sensitivity. Furthermore, the assay could be affected by regulation of protein expression on the transcriptional or the translational level. Although effects from the regulation of transcription are mitigated by a uniform cytomegalovirus (CMV) promoter, and the impact of translational regulators is reduced by the absence of 5′ and 3′ UTRs in all clones of the ORFeome library, it is nevertheless critical that the results of the GAPSA assay are confirmed and characterized using robust orthogonal approaches and validation criteria described here, including the assessment of endogenous protein activities.

The underlying goal of this study was to expand our understanding of Vpu host targets; however, we anticipate that GAPSA will provide an invaluable resource for the community that can be used to assess the regulation of protein stability on a global scale. The GAPSA platform provides a powerful tool for the global identification of molecular circuits that regulate proteostasis in the context of both physiological and disease phenotypes.

EXPERIMENTAL PROCEDURES

For a detailed description of the GAPSA platform and lists of reagents/plasmids used in this study, see Supplemental Experimental Procedures.

Cell Culture

Peripheral blood mononuclear cells (PBMCs) were isolated by Ficoll density gradient centrifugation (Histopaque, Sigma-Aldrich) from buffy coats of healthy human donors (San Diego Blood Bank). Primary human monocytes were isolated from PBMCs by positive selection for $CD14^+$ cells using CD14-MicroBeads (Miltenyi Biotec) according to the manufacturer's guidelines. Monocytes were differentiated to MDMs by culturing cells in RPMI-1640 containing 2 mM L-glutamine, 10% fetal bovine serum (FBS), 1% (v/v) HEPES (4-(2-hydroxyethyl)-1-piperazineethanesulfonic acid), 1 mM sodium pyruvate, which was supplemented with 500 U/mL granulocyte-macrophage colony-stimulating factor (GM-CSF). Medium was changed after 3 days. Cells were lifted and seeded for experiments 5 days after seeding.

$CD4^+$ T cells were isolated from PBMCs by negative selection using magnetic beads (Miltenyi Biotec). Cells were maintained in RPMI-1640 supplemented with 10% FBS, 100 IU penicillin, 100 μg/mL streptomycin, 0.1 M HEPES, 2 mM L-glutamine, and 30 U/mL interleukin-2 (IL-2). Three days before infection, cells were activated using CD3/CD28 microbeads (Thermo Fisher Scientific) according to the manufacturer's instructions.

All of the experiments involving the isolation and use of human PBMCs were conducted with approval from the institutional review board (IRB) at the Sanford Burnham Prebys Medical Discovery Institute.

cDNA Transfection and Immunoblot Assays

Transfection of cDNA constructs was conducted using a 1:5 ratio of cDNA and Fugene-6 transfection reagent (Promega), following the manufacturer's instructions. For immunoblot assays, 100 ng each of cDNA for V5-ISG and the

indicated FLAG-tagged viral accessory proteins or LacZ-FLAG were cotransfected into HEK293T cells. The cells were lysed in radioimmunoprecipitation assay (RIPA) buffer 2 days post-transfection. Protein concentrations were determined using the Pierce BCA Protein Assay Kit (Thermo Fisher Scientific) and immunoblot analysis was performed. Digitalized western blot images were uniformly adjusted for brightness and contrast using Microsoft PowerPoint. All alterations were applied equally to the entire image. Quantification of pixel intensities of bands in western blots was performed using ImageJ software version 1.46r. Relative differences in pixel intensities were calculated following the subtraction of background intensity from each pixel value.

Quantitative Real-Time PCR

Quantification of V5 and TATA binding protein (TBP) mRNA levels was performed using the ViiA7 Real-Time PCR system (Applied Biosystems). mRNA levels were normalized to TBP as reference gene. The following primers were used:

V5: 5′-CCAACTTTCTTGTACAAAGTG-3′ and 5′-TCATTACTACGTAGAATCGAGAC-3′

Virus Production and Infection Assays

HEK293T cells were seeded at 60% confluency in 10 cm plates and transfected with 20 μg of either HIV-1-Luc or HIV-1-ΔVpu-Luc plasmids using polyethylenimine (PEI) as the transfection reagent. Supernatant was collected and filtered using a 0.45 μm filter 3 days post-transfection. Similarly, vesicular stomatitis virus glycoprotein (VSV-G)-pseudotyped viruses were produced by cotransfecting 20 μg of ΔEnv proviral plasmid and 5 μg of pCMV-VSV-G. For immunoblot analysis of viral lysates, filtered supernatants from transfected cells were concentrated by centrifugation at 3000 × *g* for 16 hr at 4°C. Infectious titers of the virus stocks were determined by infecting HEK293T.CD4.CCR5 cells with varying amounts of the produced virions and analyzing Renilla luciferase reporter expression using the RenillaGlo Luciferase Assay System (PerkinElmer) 3 days post-infection. Viral p24 levels were determined using an AlphaLISA assay (PerkinElmer) according to the manufacturer's instructions.

To test the effects of HIV-1 infection on endogenous protein levels, THP-1 cells, HeLa cells, or MDMs were plated in 24-well plates at a density of 100,000 cells per well and infected with different amounts (20 or 60 ng p24 equivalent) of HIV-1-VSV-G or HIV-1-ΔVpu-VSV-G. A total of 1000 U/mL IFNβ was added to cells 48 hr after infection, where indicated. The cells were collected and lysed, and immunoblot analysis was performed 3 days post-infection.

Functional Analysis of Screen Hits

Functional analysis was conducted on 17 screen hits that were prioritized by modified *Z* score values and comprised no more than 3 hits per plate, to focus on a selection of genes that showed strong downregulation by Vpu while avoiding plate bias. Plasmids encoding V5-tagged cDNAs of selected hits (100 ng) were cotransfected into HEK293T cells together with HIV-1-Luc or HIV-1-ΔVpu-Luc plasmid (200 ng) in a 24-well format. Supernatant was collected and used to infect 20,000 HEK293T.CD4.CCR5 cells 3 days later.

V5-tagged cDNAs of CD99, PLP2, HSPA1A, and LacZ (50 or 200 ng) were cotransfected into HEK293T cells together with HIV-1-Luc or HIV-1-ΔVpu-Luc plasmid (200 ng) in a 24-well format. Supernatant was collected 3 days later and used to infect 20,000 HEK293T.CD4.CCR5 cells or $CD4^+$ T cells in a 96-well format. Infection of $CD4^+$ T cells was performed using 15 pg p24 equivalent virus. Renilla luciferase reporter expression was analyzed 3 days post-infection using the RenillaGlo Luciferase Assay System (PerkinElmer).

Viral Entry Assay

HIV-1-Luc produced in HEK293T cells ectopically expressing LacZ, CD99, or PLP2 was concentrated as described above. Viral amounts corresponding to 500 pg of p24 were used to infect 100,000 HEK293T.CD4.CCR5 cells in a 24-well format. Infection was synchronized by maintaining the cells at 4°C for 30 min before and 60 min after the addition of virus. Infection was initiated by incubating the cells at 37°C for 3 hr. Subsequently, the cells were washed 10 times with PBS to remove unbound virions and treated with trypsin for 30 min to remove virions bound to the cells. Following washes to remove excess trypsin, cells were lysed and immunoblot analysis was performed to determine p24 levels in the cells.

Generation of Stable Cell Lines and siRNA Transfection

THP-1 or HEK293T cells stably expressing UBE2L6 or vector (pLX304) alone were generated by lentiviral transduction. The respective lentiviruses were produced in HEK293T cells following standard protocols. siRNA-mediated knockdown of UBE2L6 in THP-1 cells was performed using the Stemfect RNA transfection kit (Stemgent) according to the manufacturer's protocol.

Statistical Analysis

Statistical significance was calculated in GraphPad Prism (version 7.0) using unpaired Student's t test.

SUPPLEMENTAL INFORMATION

Supplemental Information includes Supplemental Experimental Procedures, five figures, and one table and can be found with this article online at https://doi.org/10.1016/j.celrep.2018.01.091.

ACKNOWLEDGMENTS

We are grateful to Susanne Heynen-Genel and Manuel Ruidiaz (Conrad Prebys Center for Chemical Genomics [CPCCG] High-Content Screening Facility, Sanford Burnham Prebys Medical Discovery Institute) for assistance in microscopy and image data analysis, to Pedro Aza-Blanc (Functional Genomics Core Facility, Sanford Burnham Prebys Medical Discovery Institute) for assistance in cDNA cherry-picking for the screen, and to John B. Hogenesch (Cincinnati Children's Hospital Medical Center) for conceptual input. We would like to thank Kristina Herbert (Sanford Burnham Prebys Medical Discovery Institute) for critical reading of the manuscript, John Naughton (Salk Institute for Biological Studies) for providing the HEK293T.CD4.CCR5 cell line, and Nevan J. Krogan (University of California, San Francisco) for providing the FLAG-tagged constructs of Vpu, Vif, Nef, and Vpx. This study was supported by NIH/National Institute of Allergy and Infectious Diseases grants P01 AI090935, R01 AI127302, R01 AI124843, R01 AI105184, and by NIH/National Cancer Institute grant P01 CA177322 (to S.K.C.).

AUTHOR CONTRIBUTIONS

P.J., G.B., P.D.D.J., K.C.O., and S.K.C. conceived the study. P.J., P.D.D.J., K.C.O., and Q.N. conducted screening experiments. P.J., S.M.Y., L.P., and S.K.C. conducted the screen analysis. P.J., G.B., S.L., S.S., and A.J.P. conducted validation and mechanistic studies. P.J., G.B., S.L., L.P., and S.K.C. wrote the manuscript. L.P. and S.K.C. supervised the studies.

DECLARATION OF INTERESTS

The authors declare no competing interests.

Received: November 5, 2016
Revised: November 3, 2017
Accepted: January 30, 2018
Published: February 27, 2018

REFERENCES

Barr, S.D., Smiley, J.R., and Bushman, F.D. (2008). The interferon response inhibits HIV particle production by induction of TRIM22. PLoS Pathog. *4*, e1000007.

Bernard, G., Raimondi, V., Alberti, I., Pourtein, M., Widjenes, J., Ticchioni, M., and Bernard, A. (2000). CD99 (E2) up-regulates alpha4beta1-dependent T cell

adhesion to inflamed vascular endothelium under flow conditions. Eur. J. Immunol. *30*, 3061–3065.

Blanchet, F.P., Mitchell, J.P., and Piguet, V. (2012). β-TrCP dependency of HIV-1 Vpu-induced downregulation of CD4 and BST-2/tetherin. Curr. HIV Res. *10*, 307–314.

Bolduan, S., Reif, T., Schindler, M., and Schubert, U. (2014). HIV-1 Vpu mediated downregulation of CD155 requires alanine residues 10, 14 and 18 of the transmembrane domain. Virology *464-465*, 375–384.

Chan, E.Y., Qian, W.J., Diamond, D.L., Liu, T., Gritsenko, M.A., Monroe, M.E., Camp, D.G., 2nd, Smith, R.D., and Katze, M.G. (2007). Quantitative analysis of human immunodeficiency virus type 1-infected CD4+ cell proteome: dysregulated cell cycle progression and nuclear transport coincide with robust virus production. J. Virol. *81*, 7571–7583.

Chandramouli, K., and Qian, P.Y. (2009). Proteomics: challenges, techniques and possibilities to overcome biological sample complexity. Hum. Genomics Proteomics *2009*, 239204.

Der, S.D., Zhou, A., Williams, B.R., and Silverman, R.H. (1998). Identification of genes differentially regulated by interferon alpha, beta, or gamma using oligonucleotide arrays. Proc. Natl. Acad. Sci. USA *95*, 15623–15628.

Dubé, M., Paquay, C., Roy, B.B., Bego, M.G., Mercier, J., and Cohen, E.A. (2011). HIV-1 Vpu antagonizes BST-2 by interfering mainly with the trafficking of newly synthesized BST-2 to the cell surface. Traffic *12*, 1714–1729.

Goffinet, C., Allespach, I., Homann, S., Tervo, H.M., Habermann, A., Rupp, D., Oberbremer, L., Kern, C., Tibroni, N., and Welsch, S. (2009). HIV-1 antagonism of CD317 is species specific and involves Vpu-mediated proteasomal degradation of the restriction factor. Cell Host Microbe *5*, 285–297.

Goujon, C., Moncorgé, O., Bauby, H., Doyle, T., Ward, C.C., Schaller, T., Hué, S., Barclay, W.S., Schulz, R., and Malim, M.H. (2013). Human MX2 is an interferon-induced post-entry inhibitor of HIV-1 infection. Nature *502*, 559–562.

Groppelli, E., Len, A.C., Granger, L.A., and Jolly, C. (2014). Retromer regulates HIV-1 envelope glycoprotein trafficking and incorporation into virions. PLoS Pathog. *10*, e1004518.

Hahn, J.H., Kim, M.K., Choi, E.Y., Kim, S.H., Sohn, H.W., Ham, D.I., Chung, D.H., Kim, T.J., Lee, W.J., Park, C.K., et al. (1997). CD99 (MIC2) regulates the LFA-1/ICAM-1-mediated adhesion of lymphocytes, and its gene encodes both positive and negative regulators of cellular adhesion. J. Immunol. *159*, 2250–2258.

Haller, C., Müller, B., Fritz, J.V., Lamas-Murua, M., Stolp, B., Pujol, F.M., Keppler, O.T., and Fackler, O.T. (2014). HIV-1 Nef and Vpu are functionally redundant broad-spectrum modulators of cell surface receptors, including tetraspanins. J. Virol. *88*, 14241–14257.

Hrecka, K., Hao, C., Gierszewska, M., Swanson, S.K., Kesik-Brodacka, M., Srivastava, S., Florens, L., Washburn, M.P., and Skowronski, J. (2011). Vpx relieves inhibition of HIV-1 infection of macrophages mediated by the SAMHD1 protein. Nature *474*, 658–661.

Hsu, K., Han, J., Shinlapawittayatorn, K., Deschenes, I., and Marbán, E. (2010). Membrane potential depolarization as a triggering mechanism for Vpu-mediated HIV-1 release. Biophys. J. *99*, 1718–1725.

Jäger, S., Cimermancic, P., Gulbahce, N., Johnson, J.R., McGovern, K.E., Clarke, S.C., Shales, M., Mercenne, G., Pache, L., Li, K., et al. (2011). Global landscape of HIV-human protein complexes. Nature *481*, 365–370.

Kane, M., Zang, T.M., Rihn, S.J., Zhang, F., Kueck, T., Alim, M., Schoggins, J., Rice, C.M., Wilson, S.J., and Bieniasz, P.D. (2016). Identification of interferon-stimulated genes with antiretroviral activity. Cell Host Microbe *20*, 392–405.

Keshishian, H., Addona, T., Burgess, M., Kuhn, E., and Carr, S.A. (2007). Quantitative, multiplexed assays for low abundance proteins in plasma by targeted mass spectrometry and stable isotope dilution. Mol. Cell. Proteomics *6*, 2212–2229.

Kobayashi, M., Takaori-Kondo, A., Miyauchi, Y., Iwai, K., and Uchiyama, T. (2005). Ubiquitination of APOBEC3G by an HIV-1 Vif-Cullin5-Elongin B-Elongin C complex is essential for Vif function. J. Biol. Chem. *280*, 18573–18578.

Kueck, T., and Neil, S.J. (2012). A cytoplasmic tail determinant in HIV-1 Vpu mediates targeting of tetherin for endosomal degradation and counteracts interferon-induced restriction. PLoS Pathog. *8*, e1002609.

Laguette, N., Sobhian, B., Casartelli, N., Ringeard, M., Chable-Bessia, C., Ségéral, E., Yatim, A., Emiliani, S., Schwartz, O., and Benkirane, M. (2011). SAMHD1 is the dendritic- and myeloid-cell-specific HIV-1 restriction factor counteracted by Vpx. Nature *474*, 654–657.

Lama, J., Mangasarian, A., and Trono, D. (1999). Cell-surface expression of CD4 reduces HIV-1 infectivity by blocking Env incorporation in a Nef- and Vpu-inhibitable manner. Curr. Biol. *9*, 622–631.

Lee, S.Y., Kang, M.G., Park, J.S., Lee, G., Ting, A.Y., and Rhee, H.W. (2016). APEX fingerprinting reveals the subcellular localization of proteins of interest. Cell Rep. *15*, 1837–1847.

Lewinski, M.K., Jafari, M., Zhang, H., Opella, S.J., and Guatelli, J. (2015). Membrane anchoring by a C-terminal tryptophan enables HIV-1 Vpu to displace bone marrow stromal antigen 2 (BST2) from sites of viral assembly. J. Biol. Chem. *290*, 10919–10933.

Liebler, D.C., and Zimmerman, L.J. (2013). Targeted quantitation of proteins by mass spectrometry. Biochemistry *52*, 3797–3806.

Magadán, J.G., Pérez-Victoria, F.J., Sougrat, R., Ye, Y., Strebel, K., and Bonifacino, J.S. (2010). Multilayered mechanism of CD4 downregulation by HIV-1 Vpu involving distinct ER retention and ERAD targeting steps. PLoS Pathog. *6*, e1000869.

Marin, M., Rose, K.M., Kozak, S.L., and Kabat, D. (2003). HIV-1 Vif protein binds the editing enzyme APOBEC3G and induces its degradation. Nat. Med. *9*, 1398–1403.

Matheson, N.J., Sumner, J., Wals, K., Rapiteanu, R., Weekes, M.P., Vigan, R., Weinelt, J., Schindler, M., Antrobus, R., Costa, A.S., et al. (2015). Cell surface proteomic map of HIV infection reveals antagonism of amino acid metabolism by Vpu and Nef. Cell Host Microbe *18*, 409–423.

Matthews, D.R., Fruhwirth, G.O., Weitsman, G., Carlin, L.M., Ofo, E., Keppler, M., Barber, P.R., Tullis, I.D., Vojnovic, B., Ng, T., and Ameer-Beg, S.M. (2012). A multi-functional imaging approach to high-content protein interaction screening. PLoS One *7*, e33231.

Matusali, G., Potestà, M., Santoni, A., Cerboni, C., and Doria, M. (2012). The human immunodeficiency virus type 1 Nef and Vpu proteins downregulate the natural killer cell-activating ligand PVR. J. Virol. *86*, 4496–4504.

McLaren, P.J., Gawanbacht, A., Pyndiah, N., Krapp, C., Hotter, D., Kluge, S.F., Götz, N., Heilmann, J., Mack, K., Sauter, D., et al. (2015). Identification of potential HIV restriction factors by combining evolutionary genomic signatures with functional analyses. Retrovirology *12*, 41.

Ménager, M.M., and Littman, D.R. (2016). Actin dynamics regulates dendritic cell-mediated transfer of HIV-1 to T cells. Cell *164*, 695–709.

Mitchell, R.S., Katsura, C., Skasko, M.A., Fitzpatrick, K., Lau, D., Ruiz, A., Stephens, E.B., Margottin-Goguet, F., Benarous, R., and Guatelli, J.C. (2009). Vpu antagonizes BST-2-mediated restriction of HIV-1 release via beta-TrCP and endo-lysosomal trafficking. PLoS Pathog. *5*, e1000450.

Moll, M., Andersson, S.K., Smed-Sörensen, A., and Sandberg, J.K. (2010). Inhibition of lipid antigen presentation in dendritic cells by HIV-1 Vpu interference with CD1d recycling from endosomal compartments. Blood *116*, 1876–1884.

Muranyi, W., Malkusch, S., Müller, B., Heilemann, M., and Kräusslich, H.G. (2013). Super-resolution microscopy reveals specific recruitment of HIV-1 envelope proteins to viral assembly sites dependent on the envelope C-terminal tail. PLoS Pathog. *9*, e1003198.

Nazli, A., Chan, O., Dobson-Belaire, W.N., Ouellet, M., Tremblay, M.J., Gray-Owen, S.D., Arsenault, A.L., and Kaushic, C. (2010). Exposure to HIV-1 directly impairs mucosal epithelial barrier integrity allowing microbial translocation. PLoS Pathog. *6*, e1000852.

Neil, S.J., Zang, T., and Bieniasz, P.D. (2008). Tetherin inhibits retrovirus release and is antagonized by HIV-1 Vpu. Nature *451*, 425–430.

Okumura, A., Lu, G., Pitha-Rowe, I., and Pitha, P.M. (2006). Innate antiviral response targets HIV-1 release by the induction of ubiquitin-like protein ISG15. Proc. Natl. Acad. Sci. USA *103*, 1440–1445.

Pincetic, A., Kuang, Z., Seo, E.J., and Leis, J. (2010). The interferon-induced gene ISG15 blocks retrovirus release from cells late in the budding process. J. Virol. *84*, 4725–4736.

Ramirez, P.W., Famiglietti, M., Sowrirajan, B., DePaula-Silva, A.B., Rodesch, C., Barker, E., Bosque, A., and Planelles, V. (2014). Downmodulation of CCR7 by HIV-1 Vpu results in impaired migration and chemotactic signaling within $CD4^+$ T cells. Cell Rep. *7*, 2019–2030.

Ramirez, P.W., DePaula-Silva, A.B., Szaniawski, M., Barker, E., Bosque, A., and Planelles, V. (2015). HIV-1 Vpu utilizes both cullin-RING ligase (CRL) dependent and independent mechanisms to downmodulate host proteins. Retrovirology *12*, 65.

Roy, N., Pacini, G., Berlioz-Torrent, C., and Janvier, K. (2014). Mechanisms underlying HIV-1 Vpu-mediated viral egress. Front. Microbiol. *5*, 177.

Rusinova, I., Forster, S., Yu, S., Kannan, A., Masse, M., Cumming, H., Chapman, R., and Hertzog, P.J. (2013). Interferome v2.0: an updated database of annotated interferon-regulated genes. Nucleic Acids Res. *41*, D1040–D1046.

Rustagi, A., and Gale, M., Jr. (2014). Innate antiviral immune signaling, viral evasion and modulation by HIV-1. J. Mol. Biol. *426*, 1161–1177.

Salgado, C.M., Azevedo, C., Proença, H., and Vieira, S.M. (2016). Noise versus outliers. Secondary Analysis of Electronic Health Records (Springer International Publishing), pp. 163–183.

Shah, A.H., Sowrirajan, B., Davis, Z.B., Ward, J.P., Campbell, E.M., Planelles, V., and Barker, E. (2010). Degranulation of natural killer cells following interaction with HIV-1-infected cells is hindered by downmodulation of NTB-A by Vpu. Cell Host Microbe *8*, 397–409.

Sheehy, A.M., Gaddis, N.C., Choi, J.D., and Malim, M.H. (2002). Isolation of a human gene that inhibits HIV-1 infection and is suppressed by the viral Vif protein. Nature *418*, 646–650.

Shi, T., Fillmore, T.L., Sun, X., Zhao, R., Schepmoes, A.A., Hossain, M., Xie, F., Wu, S., Kim, J.S., Jones, N., et al. (2012a). Antibody-free, targeted mass-spectrometric approach for quantification of proteins at low picogram per milliliter levels in human plasma/serum. Proc. Natl. Acad. Sci. USA *109*, 15395–15400.

Shi, T., Su, D., Liu, T., Tang, K., Camp, D.G., 2nd, Qian, W.J., and Smith, R.D. (2012b). Advancing the sensitivity of selected reaction monitoring-based targeted quantitative proteomics. Proteomics *12*, 1074–1092.

Sohn, H.W., Shin, Y.K., Lee, I.S., Bae, Y.M., Suh, Y.H., Kim, M.K., Kim, T.J., Jung, K.C., Park, W.S., Park, C.S., et al. (2001). CD99 regulates the transport of MHC class I molecules from the Golgi complex to the cell surface. J. Immunol. *166*, 787–794.

Strebel, K. (2013). HIV accessory proteins versus host restriction factors. Curr. Opin. Virol. *3*, 692–699.

Sufiawati, I., and Tugizov, S.M. (2014). HIV-associated disruption of tight and adherens junctions of oral epithelial cells facilitates HSV-1 infection and spread. PLoS One *9*, e88803.

Sugden, S.M., Pham, T.N., and Cohen, E.A. (2017). HIV-1 Vpu downmodulates ICAM-1 expression, resulting in decreased killing of infected CD4+ T cells by NK cells. J. Virol. *91*, e02442-16.

Timms, R.T., Duncan, L.M., Tchasovnikarova, I.A., Antrobus, R., Smith, D.L., Dougan, G., Weekes, M.P., and Lehner, P.J. (2013). Haploid genetic screens identify an essential role for PLP2 in the downregulation of novel plasma membrane targets by viral E3 ubiquitin ligases. PLoS Pathog. *9*, e1003772.

Tripathi, S., Pohl, M.O., Zhou, Y., Rodriguez-Frandsen, A., Wang, G., Stein, D.A., Moulton, H.M., DeJesus, P., Che, J., Mulder, L.C., et al. (2015). Meta- and orthogonal integration of influenza "OMICs" data defines a role for UBR4 in virus budding. Cell Host Microbe *18*, 723–735.

Van Damme, N., Goff, D., Katsura, C., Jorgenson, R.L., Mitchell, R., Johnson, M.C., Stephens, E.B., and Guatelli, J. (2008). The interferon-induced protein BST-2 restricts HIV-1 release and is downregulated from the cell surface by the viral Vpu protein. Cell Host Microbe *3*, 245–252.

Waddell, S.J., Popper, S.J., Rubins, K.H., Griffiths, M.J., Brown, P.O., Levin, M., and Relman, D.A. (2010). Dissecting interferon-induced transcriptional programs in human peripheral blood cells. PLoS One *5*, e9753.

Wildum, S., Schindler, M., Münch, J., and Kirchhoff, F. (2006). Contribution of Vpu, Env, and Nef to CD4 down-modulation and resistance of human immunodeficiency virus type 1-infected T cells to superinfection. J. Virol. *80*, 8047–8059.

Willey, R.L., Bonifacino, J.S., Potts, B.J., Martin, M.A., and Klausner, R.D. (1988). Biosynthesis, cleavage, and degradation of the human immunodeficiency virus 1 envelope glycoprotein gp160. Proc. Natl. Acad. Sci. USA *85*, 9580–9584.

Willey, R.L., Maldarelli, F., Martin, M.A., and Strebel, K. (1992). Human immunodeficiency virus type 1 Vpu protein induces rapid degradation of CD4. J. Virol. *66*, 7193–7200.

Woods, M.W., Kelly, J.N., Hattlmann, C.J., Tong, J.G., Xu, L.S., Coleman, M.D., Quest, G.R., Smiley, J.R., and Barr, S.D. (2011). Human HERC5 restricts an early stage of HIV-1 assembly by a mechanism correlating with the ISGylation of Gag. Retrovirology *8*, 95.

Yang, X., Boehm, J.S., Yang, X., Salehi-Ashtiani, K., Hao, T., Shen, Y., Lubonja, R., Thomas, S.R., Alkan, O., Bhimdi, T., et al. (2011). A public genome-scale lentiviral expression library of human ORFs. Nat. Methods *8*, 659–661.

Yu, J., Li, M., Wilkins, J., Ding, S., Swartz, T.H., Esposito, A.M., Zheng, Y.M., Freed, E.O., Liang, C., Chen, B.K., and Liu, S.L. (2015). IFITM proteins restrict HIV-1 infection by antagonizing the Envelope glycoprotein. Cell Rep. *13*, 145–156.

Zhang, D., and Zhang, D.E. (2011). Interferon-stimulated gene 15 and the protein ISGylation system. J. Interferon Cytokine Res. *31*, 119–130.

Cell Reports, Volume *22*

Supplemental Information

Large-Scale Arrayed Analysis of Protein Degradation Reveals Cellular Targets for HIV-1 Vpu

Prashant Jain, Guney Boso, Simon Langer, Stephen Soonthornvacharin, Paul D. De Jesus, Quy Nguyen, Kevin C. Olivieri, Alex J. Portillo, Sunnie M. Yoh, Lars Pache, and Sumit K. Chanda

Figure S1.

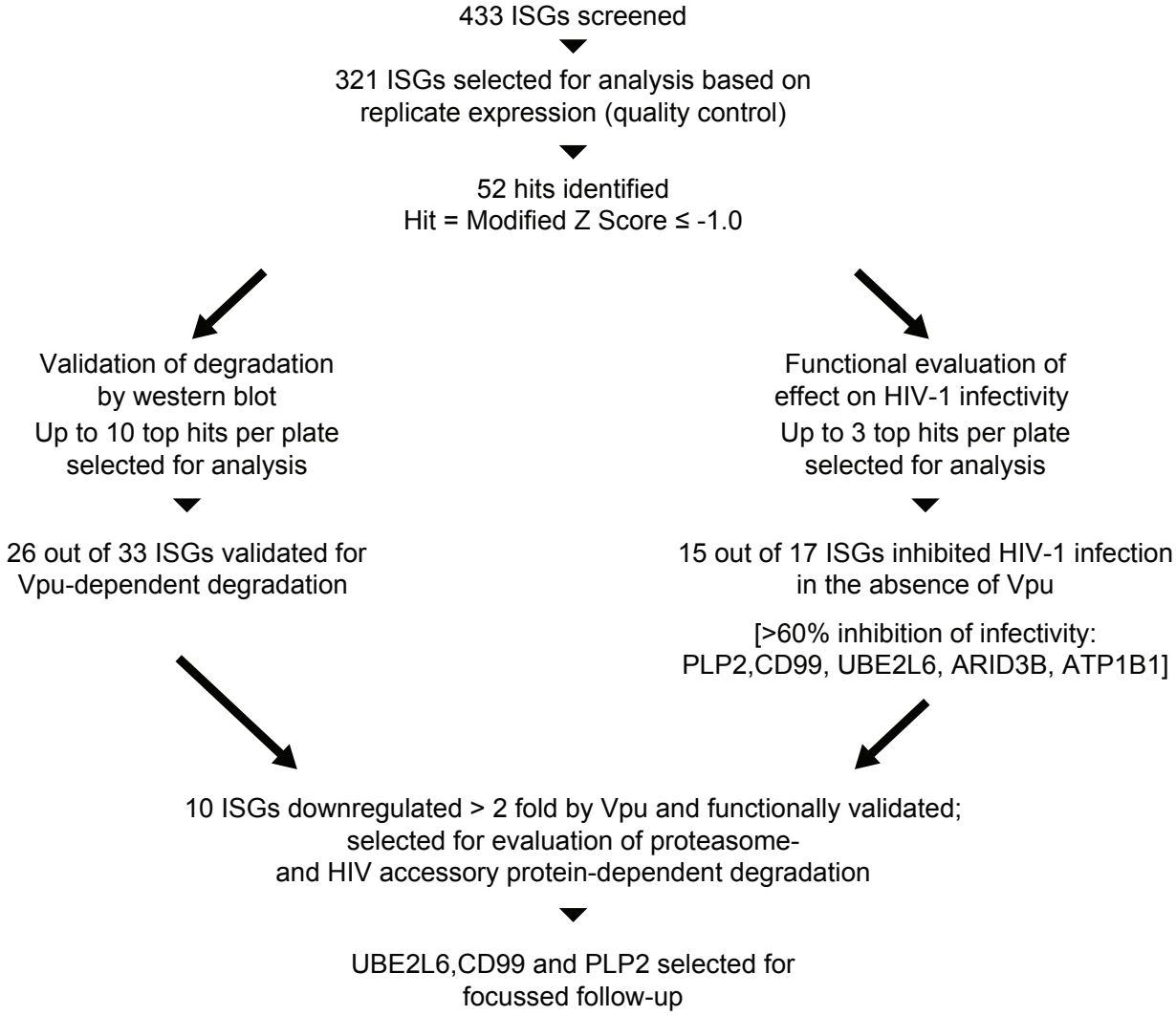

Figure S1. Schematic flowchart of hit selection, validation, and functional characterization. (*See also Figure 1A and 1D.*)

Figure S2.

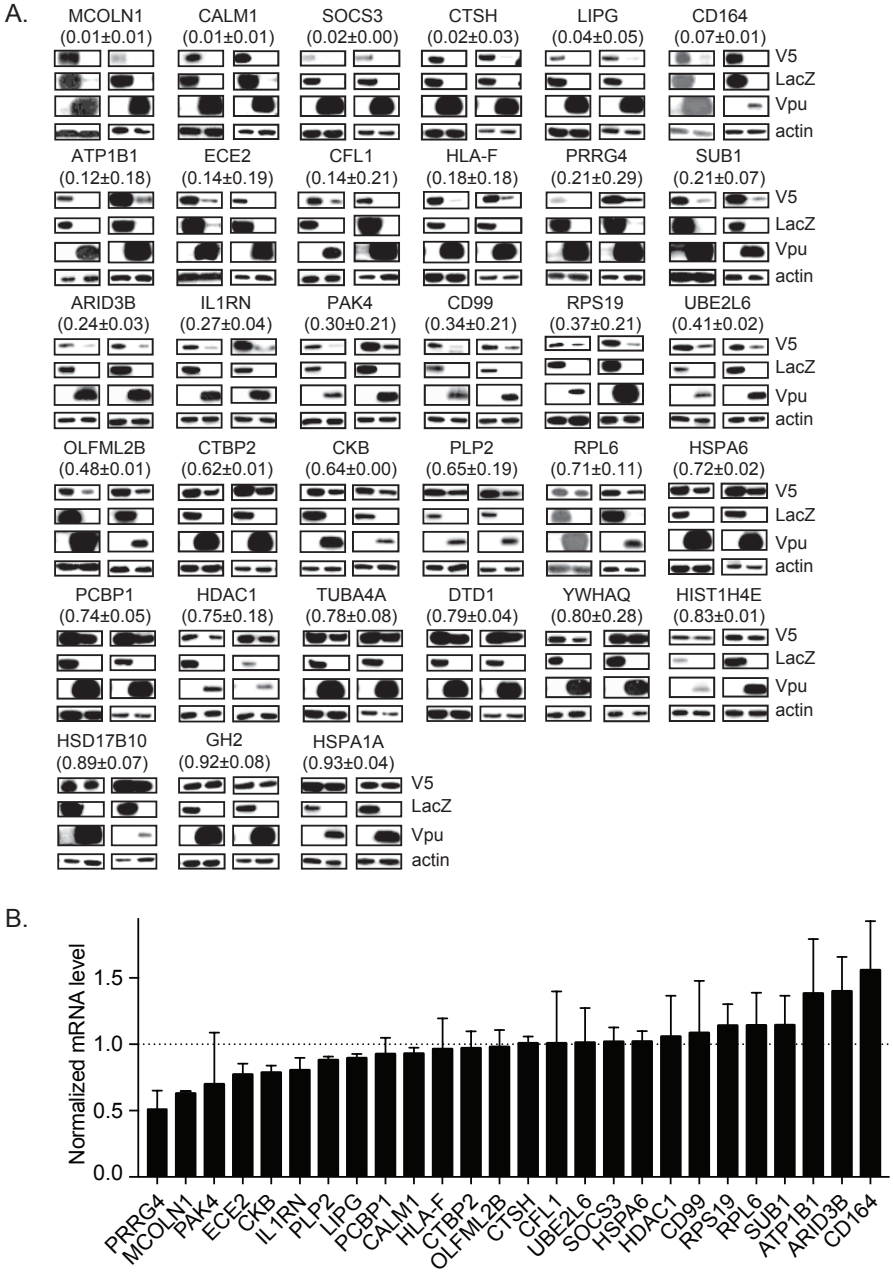

Figure S2. Evaluation of cellular ISG levels following Vpu overexpression. (*See also Figure 2A.*) (A) Whole cell lysates from HEK293T cells coexpressing Vpu-FLAG or LacZ-FLAG with indicated V5-tagged ISGs were evaluated for changes in ISG protein levels by immunoblotting and probing membranes with anti-V5 antibody and anti-FLAG antibody. Actin levels were used as loading control. Western blots from two independent experiments and average fold change values of ISG protein levels in Vpu-FLAG- versus LacZ-FLAG-expressing cells (± SD) are shown. **(B)** Changes of mRNA levels in HEK293T cells co-transfected with the indicated ISGs and Vpu relative to LacZ control. Results are represented as mean ± SD of two independent experiments.

Figure S3.

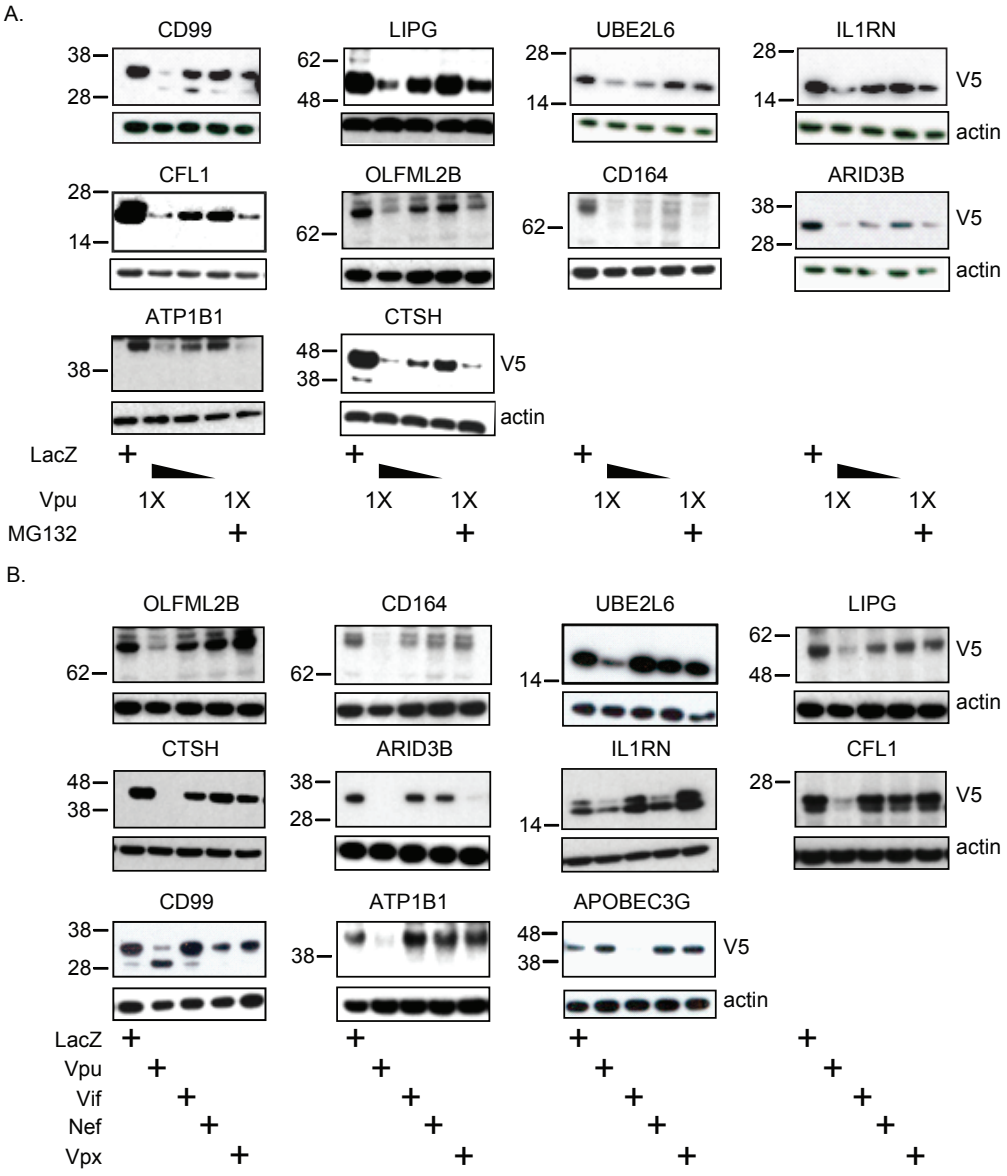

Figure S3. Evaluation of proteasome dependence and accessory protein specificity of ISG degradation. (A) (*See also Figure 3A.*) Whole cell lysates of HEK293T cells coexpressing Vpu-FLAG or LacZ-FLAG with the indicated V5-tagged ISGs in the presence or absence of MG132 were evaluated for changes in ISG protein levels by immunoblotting and probing membranes with anti-V5 antibody. Actin levels were used as loading control. Data is representative of two independent experiments. **(B) (*See also Figure 3B.*)** Whole cell lysates of HEK293T cells co-expressing FLAG-tagged Vpu, -Vif, -Nef, -Vpx or -LacZ with the indicated V5-tagged ISGs were evaluated for changes in ISG protein levels by immunoblotting and probing membranes with anti-V5 antibody. Actin levels were used as loading control. Data is representative of two independent experiments. Of note, DNA sequencing revealed that the ARID3B expression plasmid contained in the ORFeome library is a truncated form of the full-length gene.

Figure S4.

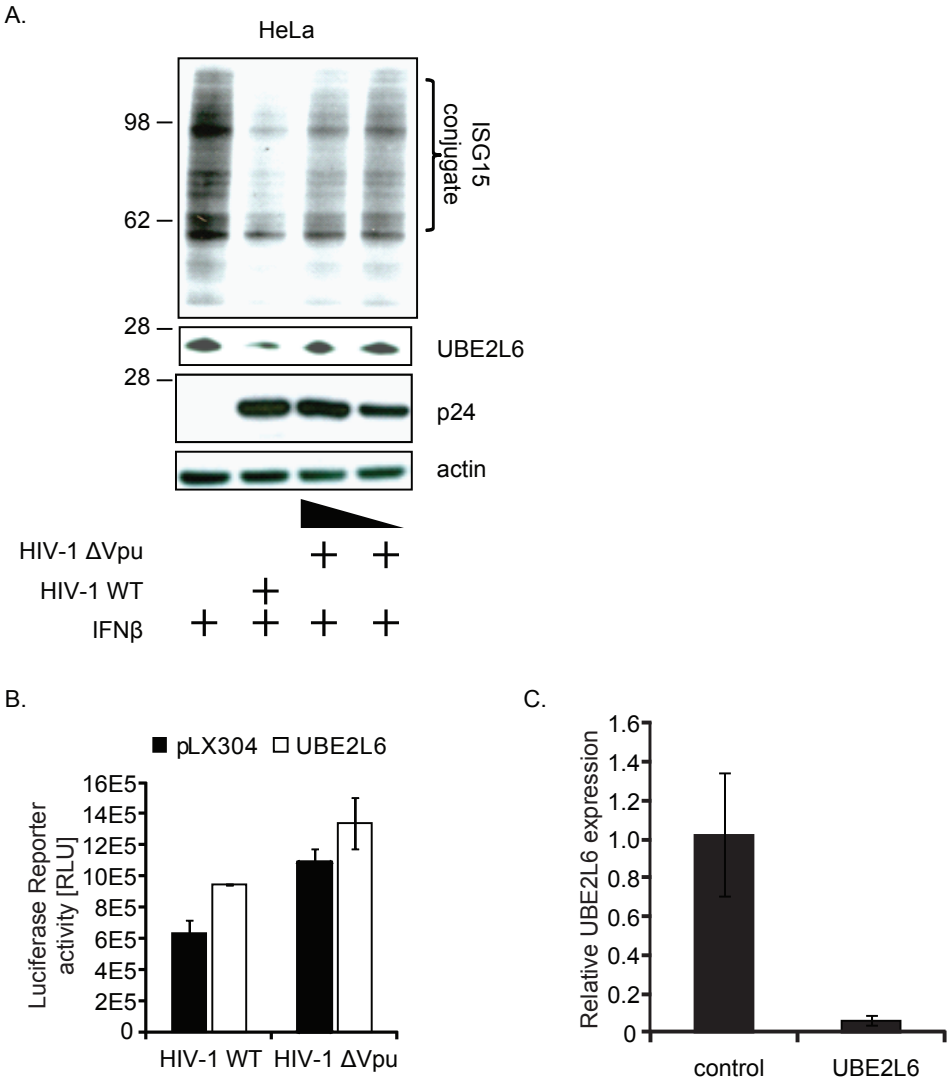

Figure S4. Vpu downregulates cellular ISGylation and endogenous UBE2L6 levels in HeLa cells. (*See also Figure 4A and 4B.*) (A) HeLa cells were infected with WT HIV-1 or Vpu-deficient HIV-1. 1000 U/ml of IFNβ was added two days post infection. Three days post infection, cells were lysed and probed for ISG15 and UBE2L6 by western blot. Intracellular p24 protein levels indicate relative infection between various treatments. Actin represents loading control. **(B) Evaluation of HIV-1 production in THP-1 cells stably expressing UBE2L6. (*See also Figure 4D.*)** *Renilla* luciferase reporter activity was measured in cells infected with comparable titers of WT or Vpu-deficient HIV-1 for three days. **(C) siRNA mediated knockdown of UBE2L6. (*See also Figure 4E.*)** Quantification of UBE2L6 mRNA levels by qPCR in THP-1 cells transfected with control siRNA (scramble) or UBE2L6 siRNA for 72 hr. Error bars indicate SD.

Figure S5.

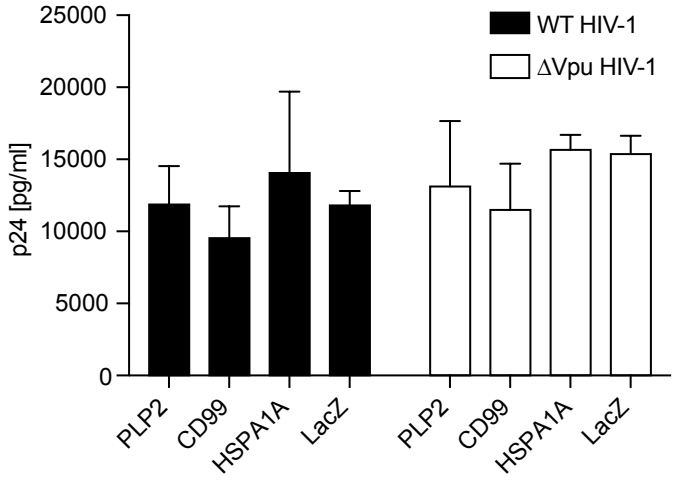

Figure S5. Intracellular p24 protein levels in producer cells are unaffected by PLP2 and CD99 overexpression. (*See also Figure 5A.*) Intracellular p24 protein levels in HEK293T cells that are co-transfected with either WT or Vpu-deficient HIV-1 and 200 ng of CD99, PLP2, HSPA1A or LacZ control. Error bars indicate SD.

Supplemental Experimental Procedures

Reagents and Plasmids

HEK293T, THP-1 and HeLa cells were purchased from ATCC (Manassas, VA). HEK293T.CD4.CCR5 cells were generously provided by John Naughton (The Salk Institute for Biological Studies). HEK293T.CD4.CCR5, HEK293T and HeLa cells were grown in DMEM (Gibco) supplemented with 10% fetal bovine serum, 1% penicillin and 100 µg/ml streptomycin. THP-1 cells were grown in RPMI-1640 (Gibco) supplemented with 10% fetal bovine serum, 1% penicillin and 100 µg/ml streptomycin.

The following reagents were obtained through the AIDS Research and Reference Reagent Program, Division of AIDS, NIAID, NIH: p24 monoclonal antibody (183-H12-5C) from Bruce Chesebro and Kathy Wehrly; HIV-1 gp120 monoclonal antibody (ID6) from Kenneth Ugen and David Weiner.

Proviral plasmids: pBR HIV-1 NL4-3 Nef IRES *Renilla* luciferase with and without *vpu* (HIV-1-Luc and HIV-1-ΔVpu-Luc), and the pBR HIV-1 NL4-3 *nef*-IRES-*Renilla* Δ*env* with or without *vpu* (HIV-1-VSV-G and HIV-1-ΔVpu-VSV-G) were previously described (Manganaro et al., 2015). pCMV-VSV-G encoding for the vesicular stomatitis indiana virus glycoprotein (VSV-G) was used to pseudotype ΔEnv viruses (Yee et al., 1994).

Expression plasmids: (pLX304) containing V5-tagged cDNAs were obtained from the Lenti ORFeome Collection (Yang et al., 2011). FLAG-tagged constructs of Vpu, Vif, Nef, and Vpx were generously provided by Nevan Krogan (University of California, San Francisco).

The following primary antibodies targeting specific proteins were used in the immunoblot assays: CD99 (Elabscience, Cat.# E-AB-11839), ARID3B (Bethyl, Cat.# A302-564A), PLP2 (Aviva Systems, Cat.# ARP45348_T100), UBE2L6 (Abgent, Cat.# AP2118b), IL1RN (R&D Systems, Cat.# AF280SP), Endothelial Lipase (LIPG) (Novus Biologicals, Cat.# NB400118SS), CFL1 (Cell Signaling Technology, Cat.# 5175), HDAC1 (Novus Biologicals, Cat.# NB100-56340SS), β-Actin (Cell Signaling Technology, Cat.# 4970s), V5 (Thermo Fisher Scientific, Cat.# MA5-15253), FLAG (Sigma, Cat.# F7425), ISG15 (Abcam, Cat.# ab14374).

Global Arrayed Protein Stability Analysis (GAPSA)

cDNA expression clones for 433 individual V5-tagged Interferon Stimulated Genes (ISGs) were obtained from the Human ORFeome V8.1 Collection (Broad Institute). cDNA concentrations were normalized to 10 ng/µl prior to spotting 2 µl using the Bravo Liquid Handling Platform (Agilent) in each well of 384-well plates (Greiner CELLSTAR, M0562) pre-coated with poly-D lysine (Sigma, P6407). 20 ng of cDNA encoding Vpu-FLAG or LacZ-FLAG, diluted in 10 µl OptiMEM (Thermo Fisher Scientific, Cat.# 11058021), were added to each well. The contents in each well were mixed by shaking the plates in microplate shaker for 30 sec. Subsequently, 0.2 µl of Fugene-6 transfection reagent (Promega, E2691) was diluted in 10 µl OptiMEM , incubated for 5 min at room temperature, and added to each well. Contents were mixed by shaking the plates in a microplate shaker for 30 sec and subsequently the plates were incubated for at least 25 min at room temperature. HEK293T cells, cultured to

approximately 60-70% confluence, were gently dislodged from flasks by incubating for 1 min with 0.05% trypsin (Sigma, 59417C). The cells were suspended in DMEM (Gibco) supplemented with 5% penicillin-streptomycin and 20% Fetal Bovine Serum at a density of $3x10^5$ cells/ml. 20 µl of the cell suspension was dispensed per well. The contents within each well were mixed by shaking the plates for 60 sec and subsequently incubated for 48 hr at 37°C and 5% CO_2 atmosphere.

Automated immunostaining protocol:

(i) PBS Wash:

96-well V bottom plates (Corning) were used as source plates for reagents. Two plates were filled with 300 µl PBS per well: 1) One source plate for PBS wash and 2) One PBS plate (dummy PBS plate) for the initial aspiration of 20 µl PBS prior to aspiration of media from the sample plate to assure pipetting accuracy. The plates were placed in Bravo stations 2 (dummy PBS plate) and 4 (PBS source plate). 250 µl tips, sample plate, and a 96 deep-well plate for waste collection were placed in Bravo stations 1, 5, and 6, respectively. A custom automated immunostaining protocol was then used to gently wash off the media from each well. The first step of the protocol involved the aspiration of 20 µl PBS from the dummy PBS plate, followed by aspiration of 20 µl media from each well and addition of 20 µl PBS from PBS source plate. This step was automatically repeated 3 times. The cells were then fixed, permeabilized, and fluorescently labeled in 4 separate automated steps, and Step 1 of the protocol described above was used before each subsequent step.

(ii) Paraformaldehyde fixation:

PBS source plate was replaced with a paraformaldehyde source plate containing 160 µl of 8% paraformaldehyde per well. The protocol was resumed to remove 20 µl PBS from each well and replaced with 20 µl of 8% paraformaldehyde from the source plate. The contents within each well were mixed by shaking the plates in a microplate shaker for 60 sec and the plates were incubated for at least 1 hr at room temperature**.**

(iii) Permeabilization:

Following a repeat of step (i), the PBS source plate was replaced with a "permeabilization solution" source plate containing 160 µl of 0.5% Triton-X100 in PBS in each well. The protocol was resumed to remove 20 µl PBS from each well and replace with 20 µl of 0.5% Triton-X100 in PBS from the source plate. The contents of each well were mixed by shaking the plates in a microplate shaker for 60 sec. The plates were then incubated for at least 10 min at room temperature**.**

(iv) Blocking of non-specific antibody binding sites:

Following a repeat of step (i), the PBS source plate was replaced with a blocking buffer source plate containing 160 µl of 6% BSA in PBS per well. 20 µl PBS was aspirated from each well and replaced with 20 µl of 6% BSA

solution from the source plate. The contents within each well were mixed by shaking the plates in microplate shaker for 60 sec prior to incubation of the plates for 1 hr at room temperature**.**

(v) Primary antibody labeling:

Following a repeat of step (i), the PBS source plate was replaced with a primary antibody source plate containing 160 µl of anti mouse-V5 and anti rabbit-FLAG antibodies at a 1:250 dilution in PBS + 6% BSA per well. 20 µl PBS was aspirated from each well and replaced with 20 µl of primary antibody solution from the source plate. The contents of each well were mixed by shaking the plates in a microplate shaker for 60 sec and subsequently incubated overnight at 4°C**.**

(vi) Secondary antibody labeling:

Following a repeat of step (i), the PBS source plate was replaced with a secondary antibody source plate containing 160 µl of goat-anti-mouse Alexa 488 and goat-anti-rabbit Alexa 568 antibodies at 1:250 dilution in PBS + 6% BSA per well. 20 µl PBS was aspirated from each well and replaced with 20 µl of secondary antibody solution from the source plate. The contents of each well were mixed by shaking the plates in a microplate shaker for 60 sec and the plates were incubated for 1 hr at room temperature**.**

(vii) Nuclei staining with DAPI:

Following a repeat of step (i), the PBS source plate was replaced with a DAPI source plate containing 160 µl of 2 µg/ml DAPI in PBS per well. 20 µl PBS was aspirated from each well and replaced with 20 µl DAPI solution from the source plate. The contents of each well were mixed by shaking the plates in a microplate shaker for 60 sec. The plates were subsequently imaged using the Opera QEHS High-Content Imaging System. Analysis of the image output was performed using the Acapella High-Content Image Analysis Software (PerkinElmer) using a custom script.

References

Manganaro, L., de Castro, E., Maestre, A.M., Olivieri, K., Garcia-Sastre, A., Fernandez-Sesma, A., and Simon, V. (2015). HIV Vpu Interferes with NF-kappaB Activity but Not with Interferon Regulatory Factor 3. Journal of virology *89*, 9781-9790.

Yang, X., Boehm, J.S., Salehi-Ashtiani, K., Hao, T., Shen, Y., Lubonja, R., Thomas, S.R., Alkan, O., Bhimdi, T., Green, T.M.*, et al.* (2011). A public genome-scale lentiviral expression library of human ORFs. Nat Methods *8*, 659-661.

Yee, J.K., Friedmann, T., and Burns, J.C. (1994). Generation of high-titer pseudotyped retroviral vectors with very broad host range. Methods Cell Biol *43 Pt A*, 99-112.